

## Accepted Manuscript

Title: Multi-dimensional optimization of the incorporation of PCM-drywalls in lightweight steel framed residential buildings in different climates

Author: N. Soares A.R. Gaspar P. Santos J.J. Costa



PII: S0378-7788(13)00789-5  
DOI: <http://dx.doi.org/doi:10.1016/j.enbuild.2013.11.072>  
Reference: ENB 4673

To appear in: *ENB*

Received date: 23-8-2013  
Revised date: 9-11-2013  
Accepted date: 25-11-2013

Please cite this article as: N. Soares, A.R. Gaspar, P. Santos, J.J. Costa, Multi-dimensional optimization of the incorporation of PCM-drywalls in lightweight steel framed residential buildings in different climates, *Energy and Buildings* (2013), <http://dx.doi.org/10.1016/j.enbuild.2013.11.072>

This is a PDF file of an unedited manuscript that has been accepted for publication. As a service to our customers we are providing this early version of the manuscript. The manuscript will undergo copyediting, typesetting, and review of the resulting proof before it is published in its final form. Please note that during the production process errors may be discovered which could affect the content, and all legal disclaimers that apply to the journal pertain.

# Multi-dimensional optimization of the incorporation of PCM-drywalls in lightweight steel framed residential buildings in different climates

N. Soares <sup>a, b, c, \*</sup>, A.R. Gaspar <sup>b</sup>, P. Santos <sup>c</sup>, J.J. Costa <sup>b</sup>

<sup>a</sup> MIT-Portugal Program, University of Coimbra - Energy for Sustainability Initiative, Coimbra, Portugal

<sup>b</sup> ADAI - LAETA, Mechanical Engineering Department, University of Coimbra, Coimbra, Portugal

<sup>c</sup> ISE, Civil Engineering Department, University of Coimbra, Coimbra, Portugal

\* E-mail address: nelson.soares@dem.uc.pt (N. Soares).

## Highlights

- !! Multi-dimensional optimization model combining EnergyPlus and GenOpt tools.
- !! Annual optimization of the incorporation of PCM-drywalls in LSF residential single-zone rooms.
- !! Quantification of the energy savings due to PCMs for seven European climates.
- !! PCM-drywalls reduce significantly the annual heating/cooling energy demands.
- !! Evaluation of the influence of the optimized solution on the energy demands throughout the year.

## Abstract

This paper evaluates the impact of PCM-drywalls in the annual and monthly heating/cooling energy-savings of an air-conditioned lightweight steel framed (LSF) residential single-zone-building, considering real-life conditions and several European climates. A multi-dimensional optimization study is carried out by combining EnergyPlus and GenOpt tools. The CondFD-algorithm is used in EnergyPlus to simulate phase-changes. For the optimization, the PSOCC-algorithm is used considering a set of predefined discrete

construction solutions. These variables are related with the thermophysical properties of the PCM (enthalpy-temperature and thermal conductivity-temperature functions), solar absorptance of the inner surfaces, thickness and location of the PCM-drywalls. Several parameters are included in the model mainly those related with the air-conditioned set-points, air-infiltration rates, solar gains, internal gains from occupancy, equipment and lighting. Indices of energy-savings for heating, cooling and for both heating and cooling are defined to evaluate the energy performance of the PCM-drywalls enhanced rooms. Results show that an optimum solution can be found for each climate and that PCMs can contribute for the annual heating/cooling energy-savings. PCM-drywalls are particularly suitable for Mediterranean climates, with a promising energy efficiency gain of about 62% for the Csb-Coimbra climate. As for the other climates considered, values of about 10% to 46% were obtained.

**Keywords:** Phase change materials, PCM, thermal energy storage, building energy simulation, light steel framing, energy efficiency, optimization.

## 1. Introduction

Lightweight steel framed (LSF) construction has been attracting interest worldwide and its popularity is increasing for use in both residential houses and apartment blocks. It presents certain advantages over heavyweight construction such as: low weight; reduced disruption on site and speed of construction; almost 100% recyclability, and architectural flexibility for retrofitting purposes. LSF construction is also particularly suited to the economy of mass production, due to a superior quality and high standards achieved by off-site manufacture control.

The main disadvantage of LSF construction can be its low thermal mass and the consequential risk of comfort problems (e.g. overheating). It is also more vulnerable to large temperature fluctuations leading to higher heating and cooling energy demands. To overcome these problems, drywalls with phase change materials (PCMs) can be incorporated allowing the building's thermal storage capacity to adapt to the needs. During the last years many global reviews that concern to PCMs and their building applications were proposed [1-16] allowing to conclude that interest on the subject is rising. In LSF construction, drywalls (also known as plasterboards, wallboards or gypsum boards) are widely used and they are very suitable for

the incorporation of microencapsulated PCMs. Many studies, numerical [17-23], experimental [24-27] or both numerical and experimental [28-36] have been carried out to assess the performance of PCM wallboards. In recent years further studies concerning the application of these elements in real buildings have been carried out in order to evaluate the influence of PCM-drywalls in more real-life conditions [37,38].

The efficiency of these elements depends on numerous factors: (i) location in the building; (ii) their volume and thermophysical properties; (iii) the phase-change temperature range; (iv) the latent heat capacity; (v) the climatic conditions; (vi) internal and solar gains; (vii) reflectivity and orientation of the surfaces; (viii) ventilation rates; (ix) HVAC controls, and (x) architectural characteristics. Therefore, the optimization of the incorporation of PCM-drywalls in LSF residential buildings is a complex task since many modelling parameters must be taken into account to realistically describe the real-life performance of the PCM enhanced building. Besides, the relationship between the set of parameters may not be simply understood due to the nonlinearity of the problem. As a result, the evaluation of the impact of alternative scenarios on the building performance requires exploring a large decision space (due to its combinatorial nature) which can be very time consuming and inefficient in a traditional iterative process.

As found by many authors, combining building energy simulation tools and optimization tools can help to optimize the design of buildings and HVAC systems in an efficient way [39-42]. Particularly, GenOpt [43] is an optimization tool that can be used for the minimization/maximization of a predefined cost function (or objective function) that is evaluated by an external building energy simulation program. Nowadays there are many building energy simulation tools. EnergyPlus [44], ESP-r [45] and TRNSYS [46] are highlighted for their versatility and reliability [47]. They are able to model PCMs for different applications in buildings as shown in works carried out using EnergyPlus [48-51], ESP-r [32,52-55] and TRNSYS [34,47,56-58]. The implemented models varied from early PCM models, to empirical models using an equivalent heat transfer coefficient, to fully implemented finite difference models and control volume models [49]. EnergyPlus PCM model uses a one-dimensional conduction finite-difference (CondFD) solution algorithm which was recently validated against multiple test suites (analytical verification, comparative testing, and empirical validation) by Tabares-Velasco *et al.* [49].

The present paper aims at evaluating the impact of PCM-drywalls in the annual and monthly heating and cooling energy savings of an air-conditioned LSF residential single-zone building (living-room),

considering real-life conditions and several European climates. To accomplish this, a multi-dimensional optimization approach is proposed by combining EnergyPlus 8.0.0 and GenOpt 3.1.0 tools. To find the optimum solution for each climate a set of discrete variables are considered in the model, namely those related with the thermophysical properties of the PCM (enthalpy-temperature and thermal conductivity-temperature functions), solar absorptance coefficient of the inner surfaces ( $\alpha$ ) and thickness and location of the PCM-drywalls. Several parameters are included in the model to better simulate real-life conditions mainly those related with the air-conditioning set-points, air infiltration rates, solar gains, internal gains from occupancy, equipment and lighting schedules.

## **2. Methodology**

### **2.1. Problem description and design variables**

In this study, the optimization of the incorporation of PCM-drywalls in LSF residential single-zone rooms in different climates is investigated. To accomplish this, a simulation-based optimization scheme is developed to account for the annual cooling and heating energy savings due to PCMs. This scheme is based on the combination of EnergyPlus with the optimization engine GenOpt. GenOpt can automatically rewrite the input files for EnergyPlus changing the independent variables considered, run the building simulation program, read (from the simulation result file) the output value of the objective function to be minimized and then determine the new set of input parameters for the next run. This iterative process is repeated until a predefined criterion of convergence is fulfilled or the maximum number of iterations is reached.

A reference air-conditioned LSF single-zone room is defined in section 2.6 for each climate presented in section 2.4. The annual heating and cooling energy demands are determined for each reference room and then compared through simulation with the total heating and cooling energy demands of the correspondent PCM enhanced room. This is attained by varying the location of the PCM-drywalls (walls and ceiling), the thickness of the elements, the melting temperature of the PCM and the  $\alpha$ -value (solar absorptance) of the inner surfaces. A set of constant parameters is used to simulate the real-life behaviour of the room (which remains constant for all case studies). These parameters are also described in section 2.6.

Therefore, the incorporation of PCM-drywalls in the LSF single-zone building is taken as a single objective multi-dimensional optimization problem. The objective function (OF)  $f: \mathbf{X} \rightarrow \mathbb{R}$  ( $f: \mathbb{Z}^{nd} \rightarrow \mathbb{R}$ ) is to

be minimized, i.e. finding  $\min_{x \in \mathbf{X}} f(x)$  subject to  $\mathbf{X} \triangleq \{x \in \mathbb{Z}^{nd} \mid x^i, i \in \{1, \dots, nd\}\}$ . The  $x \in \mathbf{X}$  is defined as

the vector of independent variables and  $\mathbf{X} \subset \mathbb{Z}^{nd}$  is the constraint set. All design solutions incorporating

PCM-drywalls are specified as discrete independent variables that can only take predefined discrete values

defined in  $\mathbb{Z}^{nd}$ . These predefined construction solutions are function of the melting peak temperature of the

PCM ( $T_{pm}$ ), thickness of the PCM-drywall ( $e_{PCM}$ ) and  $\alpha$ -value of the inner surfaces. Six PCM-drywalls with melting peak temperatures of 18, 20, 22, 24, 26 and 28 °C are considered for the optimization problem. The  $e_{PCM}$ -value can assume one of the seven possible values: 1.0, 1.5, 2.0, 2.5, 3.0, 3.5 and 4.0 cm. The  $\alpha$ -value is related with the colour of the surface (or selective inks can be used) and it can be equal to 0.3, 0.5, 0.7 or 0.9. Regarding the combination of all referred values, a set of 169 predefined discrete solutions can be considered (reference solution + 6 PCMs  $\times$  7  $e_{PCM}$ -values  $\times$  4  $\alpha$ -values).

Five categories of enhanced surfaces with PCM-drywalls are involved in the optimization problem: external southern ( $S$ ), western ( $W$ ) and eastern ( $E$ ) walls; northern partition wall ( $N$ ) and ceiling ( $C$ ).  $S$ ,  $W$ ,  $E$ ,  $N$  and  $C$  represent the set of predefined admissible discrete solutions for each corresponding surface. Hence, this optimization setup is five-dimensional ( $nd = 5$ ). Constraint sets for the independent variables are defined

as  $x^1 = \{S_j, j \in \{0, \dots, 169\}\}$ ,  $x^2 = \{W_k, k \in \{0, \dots, 169\}\}$ ,  $x^3 = \{E_l, l \in \{0, \dots, 169\}\}$ ,  $x^4 = \{N_m, m \in \{0, \dots,$

$, 169\}\}$ , and  $x^5 = \{C_p, p \in \{0, \dots, 43\}\}$ . Vector  $C$  has only 43 admissible values since the solar absorptance of

the ceiling is kept constant and equal to 0.3.

## 2.2. Optimization approach

The OF to be minimized (Eq. 1) for each climate is based on the annual heating and cooling energy savings from the replacement of the inner gypsum plasterboard layer of the reference surfaces by a PCM-drywall.  $E_{\text{heat,ref,a}}$  and  $E_{\text{cool,ref,a}}$  are the annual energy demand for heating and cooling, respectively, derived from the simulation of the reference room.  $E_{\text{heat,PCM,a}}$  and  $E_{\text{cool,PCM,a}}$  are also predicted by simulation and correspond to the annual energy demand for heating and cooling, respectively, after including PCM-drywalls

in the model. For each optimization problem, with the corresponding weather data,  $x^* \in \mathbf{X}$  denotes the

iterated solution with the lowest cost function value. It can also be defined as  $x^* = \{S_j, W_k, E_l, N_m, C_p\}_{\text{opt}}$ .

$$OF(x) = E_{\text{heat, PCM, a}}(x) + E_{\text{cool, PCM, a}}(x) + E_{\text{heat, ref, a}} + E_{\text{cool, ref, a}} \quad (1)$$

The efficiency and success of an optimization process is strongly affected by the properties and the formulation of the OF, and by the selection of an appropriate optimization algorithm [59]. The full enumeration (exhaustive search) of the design parameter spaces requires more than  $35 \times 10^9$  EnergyPlus simulation runs, corresponding to 43 ceilings  $\times$  169 southern  $\times$  169 western  $\times$  169 eastern  $\times$  169 northern walls. To avoid looking for the independent variables that yield better performance in the entire design parameter space (very time consuming), the particle swarm optimization algorithm with constriction coefficient (PSOCC) described in [59] is used.

Particle swarm optimization (PSO) algorithms are from a family of meta-heuristic population-based and stochastic optimization techniques first proposed by Kennedy and Eberhart [60,61]. At each iteration step, PSO compares the cost function value of a finite set of points, called particles. The set of potential solutions (particles) is called a population. The next populations are computed using a particle update equation. As summarized by Wetter and Wright [39], the change of each particle from iteration to iteration is modelled based on the social behaviour of flocks of birds or schools of fish. Each particle attempts to change its location in  $\mathbf{X}$  source to a point where it had a lower cost function value at previous iterations (cognitive behaviour modelling), and in a direction where other particles had a lower cost function value (social behaviour modelling) [39]. In this study, the simulation model is computationally expensive due to the big dimension of the vectors that describe the possibilities for each discrete variable. PSOCC algorithm is used with the *von Neumann* neighbourhood topology, a population size of 25 particles with a maximum of 1500 generations, a seed of 1, a cognitive acceleration constant of 2.8, a social acceleration constant of 1.3, a velocity clamping with a maximum velocity gain of 4 and a constriction gain of 0.5.

### 2.3. Performance indicators: indices of energy savings

Three indices are defined to evaluate the energy performance of the PCM-drywall enhanced room, namely the indices of energy savings for heating ( $IESH_i$ ), for cooling ( $IESC_i$ ) and for both heating and cooling ( $IEST_i$ ), respectively defined as:

$$IESH_i = 1 - E_{\text{heat, PCM, } i} / E_{\text{heat, ref, } i}, \quad i = a, m \quad (2)$$



$$IESC_i = 1 - E_{cool,PCM,i} / E_{cool,ref,i}, i = a, m \quad (3)$$

$$IEST_i = 1 - E_{tot,PCM,i} / E_{tot,ref,i}, i = a, m \quad (4)$$

where,  $E_{tot,ref,i}$  and  $E_{tot,PCM,i}$  are the total energy demand for heating and cooling considering the reference room and the PCM-drywalls enhanced room, respectively. Subscript  $i$  refers to time period assessment. The subscripts  $a$  and  $m$  correspond to the annual and the monthly assessment basis, respectively.

#### 2.4. Characterization of the European climates

Seven climate files provided by the International Weather for Energy Calculation (IWEC) [44] for different cities were considered to cover the main European climatic regions according to the Köppen-Geiger classification [62]. The European climates were divided into two main groups, warm temperate (C) and snow (D), and several subtypes regarding average values of precipitation - fully humid (f) and summer dry (s) - and temperatures - hot summer (a), warm summer (b) and cool summer (c). Table 1 presents the Köppen-Geiger classification and the description of the seven reference climates selected for this study. Basically, the European climates change with latitude, altitude and coast vicinity. In southern Europe, the climate of regions with lower latitudes (below 45°N) is generally classified as Csa and Csb. Above these latitudes (between 45-55°N) the climate is mainly labelled as Cfb and Dfb, for western and eastern central European countries, respectively. In Northern Europe, in regions with latitudes above 55°N, the climate is typically classified as Dfc.

#### 2.5. EnergyPlus PCM model

EnergyPlus 8.0.0 includes the CondFD model proposed by Pederson [51] and improved by Tabares-Velasco *et al.* [49]. It is an implicit finite difference scheme coupled with an enthalpy-temperature function to account for phase change energy accurately. Eq. (5) represents the implicit formulation for an internal node:

$$!c_p ! x \frac{T_{i,new} - T_{i,old}}{! t} + k_{int} \frac{T_{i+1,new} - T_{i,new}}{! x} + k_{ext} \frac{T_{i+1,new} - T_{i,new}}{! x} \quad (5)$$

where

$$k_{int} = \frac{k_{i+1,new} + k_{i,new}}{2} \quad (6)$$

$$k_{ext} = \frac{k_{i-1,new} + k_{i,new}}{2} \quad (7)$$

Subscripts refer to nodes and applicable time step. The *new* and *old* time steps are the present and the previous time steps, respectively. The node  $i$  is the node being modelled and the nodes  $i+1$  and  $i-1$  are the adjacent nodes to the inner and outer sides of the construction, respectively. The space between nodes used as the finite difference layer thickness is denoted  $\Delta x$ . In the CondFD algorithm, all elements are discretized using Eq. (8) which depends on a space discretization constant ( $c$ ), the thermal diffusivity of the material ( $\alpha^*$ ), and the time step ( $\Delta t$ ). Eq. (8) can also be written as function of the Fourier number ( $Fo$ ):

$$\Delta x = \sqrt{c \alpha^* \Delta t} = \sqrt{\frac{\alpha^* \Delta t}{Fo}} \quad (8)$$

Eq. (5) is coupled by Eq. (9) and Eq. (10) that relate the enthalpy ( $h$ ) and the thermal conductivity ( $k$ ) of the PCM with the temperature ( $T$ ), respectively.

$$h_i = h(T_{i,new}) \quad (9)$$

$$k_i = k(T_{i,new}) \quad (10)$$

An equivalent variable specific heat ( $c_{p,eq}$ ) at each time step can be defined as:

$$c_{p,eq} = \frac{h_{i,new} - h_{i,old}}{T_{i,new} - T_{i,old}} \quad (11)$$

In a recent work, Tabares-Velasco *et al.* [49] identified some guidelines for using the EnergyPlus PCM model. They found that time steps equal to or shorter than three minutes should be used. They also stated that the default CondFD model can be used with acceptable monthly and annual results ( $Fo = 1/3$  and  $c = 3$ ). However, if accurate hourly performance and analysis is required, smaller node space (1/3 of the default value) should be used at the expense of longer run times. In this study, the CondFD default model with 20 time steps per hour ( $\Delta t$  equal to three minutes) is used for the monthly and annual analysis of the heating and cooling energy demands (for both the reference and the PCM-enhanced rooms).

As stated above, the EnergyPlus PCM model requires an enthalpy-temperature function and a thermal conductivity-temperature function, both using data supplied as input. These functions are not linear for most PCMs and frequently not known in detail. Furthermore, obtaining these data could be challenging because careful selection of heating/cooling rates and calibration of instrumentation are needed [50]. In his

recent work, Tabares-Velasco [50] investigated the energy impacts of nonlinear behaviour of enthalpy-temperature functions considering the CondFD model. The author stated that a linear function could facilitate parametric and optimization analysis as well as broad analyses that would design generic PCMs that manufactures could later produce following specific guidelines [50]. He concluded that annual energy savings are not very sensitive to the linearization of the enthalpy-temperature curve. For hourly analysis, the simpler linear profiles should be specified in a way that the melting range covers roughly 80% of the latent heat, otherwise, hourly results can differ by up to 20% [50].

In the present work, the energy impacts of linear enthalpy-temperature functions are considered for microencapsulated PCMs distributed in drywalls. The DuPont™ Energain® PCM product was considered as a reference PCM-drywall. This material has a nonlinear enthalpy-temperature function, a melting temperature range centred around 21.7 °C, a latent heat of 70 kJ/kg, a density of 855 kg/m<sup>3</sup>, a specific heat of 2500 J/kg K and a variable thermal conductivity [49]. Based on the nonlinear enthalpy-temperature function of the reference material (PCMref), a new linear function was plotted for a hypothetical material (PCM22) with the melting range covering roughly 80% of the latent heat (Fig. 1a). This new material has a melting temperature range between 18 °C and 26 °C centred around 22 °C. Five other hypothetical materials with the same latent heat characteristics were further defined to investigate the impact of different melting peak temperatures. Therefore, six PCM-drywalls with different melting peak temperatures are considered in the optimization problem. Fig. 1a and Fig. 1b show, respectively, the enthalpy-temperature and the thermal conductivity-temperature functions for the reference PCM-drywall and for the other six hypothetical materials defined.

The EnergyPlus PCM model described above does not simulate hysteresis of the PCM and only the enthalpy-temperature information for the heating mode is inputted. Therefore, as found by Tabares-Velasco *et al.* [49], accuracy issues can arise when modelling PCMs with strong hysteresis. Hence, for the purpose of this work, the hysteresis phenomenon was not considered in the simplified model. Another limitation of the EnergyPlus PCM model is that variations of the PCM density cannot be modelled to account for changes in volume during phase transitions. The heat transfer by convection cannot be simulated using the pure diffusion EnergyPlus PCM model as well. This is not critical for problems of microencapsulated PCMs dispersed in gypsum boards, but it is particularly critical when nonmicroencapsulated organic PCMs are

incorporated in envelope solutions. In these cases, a macrocapsule is normally considered to avoid leakage, and the heat transfer by convection and the volume variations must be considered in the model. For the purpose of this study, the density value is assumed constant and no changes in volume are considered.

## 2.6. Reference rooms

For each climate considered, a reference room is defined based on an air-conditioned LSF residential single-zone (living room) with dimensions: 8 m wide  $\times$  6 m long  $\times$  2.7 m high (Fig. 2). The reference room looks very similar to the one specified in ASHRAE 140 standard [64]. The total floor area of the room is 48 m<sup>2</sup> with a slab-on-grade foundation. The model is perfectly east-west oriented with a total window area of 12 m<sup>2</sup> on the south façade ( $G = 0.7$ ). For an efficient use of solar heat gains, windows are provided with an external movable shading device (horizontal blinds with high reflectivity slats). From October to May, blinds are pulled back during the day to maximize solar gains (from 8 am to 6 pm). During the night (from 6 pm to 8 am) blinds are lowered and closed to reduce heat losses through the windows (slat angle set to 3°). From June to September, blinds are lowered with slats set to 90° during the day (from 8 am to 8 pm) to reduce solar gains. During summer nights blinds are retracted (from 8 pm to 8 am). Concerning boundary conditions, all vertical surfaces are considered external walls except the northern surface, which is a partition wall. For this surface, an adiabatic boundary condition is considered assuming that no heat exchanges occur between the living room and the other building zones (Fig. 2). The existence of interior doors is also neglected in the simplified model.

Regarding internal heat gains, the living room is occupied by a maximum of 4 people in sedentary activity with a constant metabolic rate of 1.2 met (126 W/person). To simulate a real-lifestyle, the room is considered occupied during the weekend days and weekday evenings. The maximum heat loads due to equipments and lighting are 400 W and 120 W, respectively. Fig. 3. shows the occupancy, lighting and equipment schedules considered in the model. The reference rooms are air-conditioned considering an ideal loads air system model (in the EnergyPlus simulations) to obtain the rooms thermal loads. When the living room is occupied, the thermostat is set with a dead band so heating takes place for temperatures below 20 °C and cooling for temperatures above 25 °C. When the room is not occupied, the air temperature heating and cooling set-points are set to 15 °C and 30 °C, respectively. An infiltration rate of 0.5 air changes per hour is

considered in the simulations. During summer nights (from June to September), when the room is empty (from 1 am to 8 am), a ventilation rate of 1.5 air changes per hour is also considered.

Generally speaking, there are three design types of LSF constructions: cold frame construction; warm frame construction, and hybrid construction. In this study a hybrid framed construction is adopted with insulation tightly fitted between the steel studs in addition to insulation at the external side of the studs. Fig. 4 illustrates the cross-sections of the LSF walls (Fig. 4a), roof (Fig. 4b), slab-on-grade (Fig. 4c) and partition walls (Fig. 4d). Hybrid construction differs from cold frame constructions because in the latter, all the insulation is included within the thickness of the steel components and the steel members entirely bridge the insulation layer. Therefore, this construction has a higher degree of thermal bridging. In warm frame construction all the insulation is outside the steel framing [65]. Table 2 lists the thermophysical properties of the materials considered in this study.

The set of parameters described above prevails for all the reference rooms. Variations in thermal insulation standards are to be expected from the north to the south European countries. In fact, the maximum  $U$ -value of the envelope elements are fixed by the building regulations of each country [66] as the result of the implementation of the Energy Performance of Buildings Directive (EPBD) by each state. In this work, different reference  $U$ -values are considered for the exterior walls, roof and windows of each climate as shown in Table 3. The reference  $U$ -values are considered equal to the correspondent maximum  $U$ -values specified in the regulations of each country [66]. In section 2.7 a simplified method for calculating  $U$ -values of LSF construction elements is described to account for thermal bridging effect.  $U$ -values are obtained by varying the thickness of the outer insulation layers,  $e_{\text{ins,wall}}$  and  $e_{\text{ins,roof}}$  (Fig. 4). In the PCM-drywalls enhanced building, the inner plasterboard layers of the exterior walls, roof and partition wall are replaced by a PCM-drywall layer as explained in section 2.2.

### **2.7. $U$ -values in light steel framing and thermal bridging in EnergyPlus**

The effects of non-homogenous layers and thermal bridges (when the difference between the thermal conductivity of materials is large) should be considered in the calculation of the  $U$ -value of LSF elements [67]. Indeed, depending on the details of the construction, ignoring the effect of the steel can lead to an overestimate of the thermal resistance by up to 50% [68]. In this section, a simplified method to account for

thermal bridging effects in EnergyPlus simulations is presented. A fictitious equivalent material is defined to replace the heterogeneous layer composed by insulation and steel frames. The thermal conductivity of the equivalent layer material is adjusted for each climate so that the effective thermal resistance is equal to that of the insulation panel with metallic frames.  $U$ -values listed in Table 3 are used to determine the equivalent thermal conductivities. The density and the specific heat of these equivalent materials are also adjusted to match the thermal capacity of the insulation with metal frames according to Eqs. (12) and (13), respectively.

$$\rho_{eq} = \sum_{i=1}^n \rho_i \phi_i \quad (12)$$

$$c_{p,eq} = \frac{1}{\rho_{eq}} \sum_{i=1}^n \rho_i \phi_i c_{p,i} \quad (13)$$

where:  $\rho_{eq}$  is the density of the equivalent layer ( $\text{kg/m}^3$ );  $\rho_i$  is the density of the material  $i$  ( $\text{kg/m}^3$ );  $\phi_i$  is the volumetric fraction of the material  $i$ ;  $c_{p,eq}$  is the specific heat of the equivalent layer ( $\text{J/kg K}$ ) and,  $c_{p,i}$  is the specific heat of the material  $i$  ( $\text{J/kg K}$ ).

Table 4 lists the values of the thermal conductivity of the equivalent homogeneous layer materials for each climate. Considering the exterior and partition walls elements, the density and the specific heat of the equivalent homogeneous material are equal to  $116 \text{ kg/m}^3$  and  $549.7 \text{ J/kg K}$ , respectively, for all the climates. As for the exterior roof elements, these values are  $123 \text{ kg/m}^3$  and  $544 \text{ J/kg K}$ , respectively.

The simplified method of calculating  $U$ -values in LSF hybrid construction proposed in [65,68] is used in this work. This method is similar in principle to that used in BS EN ISO 6946 [69] but adapted to increase accuracy for hybrid LSF construction. It was found by Gorgolewski [68] that with the proposed method the mean error of prediction compared with finite element modelling is less than 3% with a maximum error of 8% for a range of 52 assessed constructions.

The method involves the calculation of the upper and lower limits of thermal resistance. The upper limit of thermal resistance ( $R_{max}$ ) is calculated by combining in parallel the total resistances of the heat-flow paths through the building element (thermal paths (a) and (b) illustrated in Fig. 4). The conductance associated with  $R_{max}$  is calculated by combining the conductance through paths (a) and (b) (Fig. 4) on an area-weighted basis. The lower limit of thermal resistance ( $R_{min}$ ) is calculated by combining in parallel the resistances of the heat flow paths of each layer separately and then summing the resistances of all layers of the building element. The conductance of the bridged layer is also calculated on an area-weighted basis. The

fraction of the area taken up by the webs of the steel studs, noggins and braces adds up to 0.56% and 0.76% for the exterior walls and roof, respectively. The internal surface resistance ( $R_{si}$ ) is equal to 0.13 m<sup>2</sup>K/W (horizontal heat flow) or 0.10 m<sup>2</sup>K/W (heat flow upwards). The external surface resistance ( $R_{se}$ ) is equal to 0.04 m<sup>2</sup>K/W (horizontal or upwards heat flow). The  $U$ -value is calculated by

$$U = 1/R_T \quad (14)$$

where the total thermal resistance ( $R_T$ ) is obtained by

$$R_T = pR_{max} + (1-p)R_{min} \quad (15)$$

The  $p$ -value is calculated according to Eq. (16) and it is influenced by several factors, including the flange width, the spacing between studs ( $s$ ) and the depth of the stud ( $d$ ). The  $s$ -value and the  $d$ -value in Eq. (16) must be expressed in mm. Eq. (16) is valid when the flange widths are known not to exceed 50 mm. It should be remarked that only the webs of the steel studs, noggins and braces are included in the calculation of  $R_{max}$  and  $R_{min}$  as the effects of the flanges are taken into account in the formula for  $p$ .

$$p = 0.8 \frac{R_{min}}{R_{max}} + 0.32 + 0.2 \frac{600}{s} + 0.04 \frac{d}{100} \quad (16)$$

The  $U$ -value corrections for air gaps and fixings proposed in [68] are not considered in this work because the design consists of two layers of insulation (one between studs, the other as a continuous layer covering the first one) and plastic fixings are used in the steel flanges to attach the studs to the external sheathing board.

### 3. Results and discussion

#### 3.1. Annual assessment basis

In this section, the results of the annual assessment of the energy savings for heating and cooling are presented. Table 5 shows the values of the independent variables that yield better performance for each climate (lowest cost function value). It can be seen that a 4.0 cm PCM-drywall is the optimum thickness for all the surfaces (considering the set of  $e_{PCM}$ -values analysed). The optimum  $T_{pm}$ -value is different regarding the orientation of the surface and the climate considered. Generally speaking, the  $T_{pm}$ -value is lower for the partition wall than for the other surfaces. The  $T_{pm}$ -value is higher for the warmer climates and lower for the colder climates. Concerning the optimum  $\alpha$ -value, it also varies according to the orientation of the surface and the climate. Inner surfaces with higher  $\alpha$ -value are better for colder climates. Table 6 lists the annual

heating and cooling energy demands of the reference room and the PCM-drywalls enhanced room, for each climate. It also lists the annual heating and cooling energy savings considering the optimized solution  $x^*$ .

Fig. 5 shows the annual heating and cooling energy demands for both the reference and the PCM-enhanced rooms for each climate and the associated indices of annual energy savings. The bars in greyscale correspond to the heating and cooling energy demands (read on the left axis) for the reference room for each climate. Next to each of these, the coloured bars correspond to the PCM-enhanced room energy demands for the same climate. Additionally, the bullets on the graph indicate the indices of annual energy savings (read on the right axis) for each climate. The  $IESHa$  varies between 0.07 (Dfc-Kiruna) and 0.92 (Csa-Seville);  $IESCa$  between 0.43 (Csa-Seville) and 0.87 (Dfc-Kiruna); and  $IESta$  varies between 0.10 (Dfc-Kiruna) and 0.62 (Csb-Coimbra). Therefore, results show that the energy performance of LSF air-conditioned residential buildings can be significantly improved with the incorporation of PCM-drywalls in all the climates evaluated.

This impact is more significant for the warmer climates where the total energy savings for both heating and cooling reach 46% (38.23 kWh/m<sup>2</sup> year) and 62% (28.74 kWh/m<sup>2</sup> year) for the Csa-Seville and Csb-Coimbra climates, respectively. This is particularly due to the reduction in the energy consumption for cooling, i.e. 43% (33.94 kWh/m<sup>2</sup> year) and 61% (24.78 kWh/m<sup>2</sup> year) for the Csa-Seville and Csb-Coimbra climates, respectively. For these climates the reference energy demand is lower for heating than for cooling. However, the optimized incorporation of PCM-drywalls in the model also reduces significantly the heating energy demand, i.e. 92% (4.3 kWh/m<sup>2</sup> year) and 70% (3.95 kWh/m<sup>2</sup> year) for the Csa-Seville and Csb-Coimbra climates, respectively.

Regarding colder climates (Dfb-Warsaw and Dfc-Kiruna), the impact of PCM-drywalls in the total energy savings is not so significant, i.e. 24% (13.68 kWh/m<sup>2</sup> year) and 10% (9.86 kWh/m<sup>2</sup> year) for the Dfb-Warsaw and Dfc-Kiruna climates, respectively. This is particularly due to the decrease in the energy demand for heating, i.e. 13% (6.34 kWh/m<sup>2</sup> year) for the Dfb-Warsaw and 7% (6.58 kWh/m<sup>2</sup> year) for the Dfc-Kiruna climates. Another attractive result is that the optimized incorporation of PCM-drywalls in the room significantly reduces the cooling energy demand, i.e. 74% (7.34 kWh/m<sup>2</sup> year) and 87% (3.28 kWh/m<sup>2</sup> year) for the Dfb-Warsaw and Dfc-Kiruna climates, respectively.



Concerning the other climates (Cfa-Milan, Cfb-Paris and Dfa-Bucharest), results show that the optimum incorporation of PCM-drywalls in the room reduces both the annual energy demand for cooling and heating. The index  $IESHa$  varies between 0.19 (Cfb-Paris) and 0.25 (Dfa-Bucharest);  $IESCa$  between 0.45 (Cfa-Milan) and 0.72 (Cfb-Paris), and  $IESta$  between 0.33 (Cfa-Milan) and 0.38 (Dfa-Bucharest). Therefore, for these climates, the energy savings are particularly due to the reduction in the energy demand for cooling.

### 3.2. Monthly assessment basis

In this section results of the monthly assessment of the energy savings for heating and cooling are presented to show the impact of the annual optimized solution  $x^*$  on the energy demands throughout the year. Fig. 6 shows the monthly heating and cooling energy demands for both the reference and the PCM-enhanced rooms for each climate analysed. It also shows the indices of energy savings for each month (for each climate) considering the optimized solution  $x^*$ . The bars in greyscale correspond to the heating and cooling energy demands (read on the left axis) for the reference room. Next to each of these, the coloured bars correspond to the PCM-enhanced room energy demands for the same month. Additionally, the bullets on the graph indicate the indices of energy savings (read on the right axis) for each month. Table 7 lists the monthly heating and cooling energy savings for the analysed climates considering the optimized solution  $x^*$ .

To prevent this paper from becoming too long, only the graphs of Fig. 6a and Fig. 6g will be discussed in detail. These graphs concern to the warmer (Csa-Seville) and colder (Dfc-Kiruna) climates, respectively. For the Csa-Seville climate (see Fig. 6a), the energy demand in summer is due to cooling. During this season, the cooling and the total energy savings due to PCMs vary both between 25% in July and 37% in June. The  $IESHm$  is not defined during summer because no heating is required. Regarding the swing seasons (spring and autumn), the optimized incorporation of PCM-drywalls almost eliminates heating demands (savings from 92% in November to 100% in March, May, September and October), and leads to cooling savings between 29% in September and 62% in November. The total energy savings vary between 29% in September and 65% in November. During winter, the heating savings range from 86% in December to 94% in February; the cooling savings from 76% in February to 81% in December; and the total energy savings vary between 79% in February and 82% in January. January is the month with the highest level of total energy savings, i.e. 4.43 kWh/m<sup>2</sup> (see Table 7).

Regarding warmer climates, most studies found in literature deal with the optimization of the incorporation of PCM-drywalls for summer without assessing the impact of the latent heat loads in the remaining seasons [48,55]. For the Csa-Seville climate, results show that PCM-drywalls can also have a significant impact in the reduction of the heating and cooling energy demands during the swing seasons and winter. Therefore, high levels of energy reduction occur from January to March and from October to December, as it can be seen in Table 7. These results are explained by the extra thermal capacity of the envelope provided by the incorporation of PCMs.

The energy demands for the Dfc-Kiruna climate (see Fig. 6g) is mainly due to heating during winter and swing seasons. Nevertheless, a remaining energy demand is required for cooling during summer, which is significantly reduced with the optimized solution:  $IESC_m$  between 0.87 in August and 0.99 in June;  $IESH_m$  between 0.61 in June and 0.99 in July; and  $IEST_m$  between 0.63 in August and 0.93 in July. During the swing seasons the total energy savings vary from 3% in November to 86% in May; the heating savings from 3% in November to 98% in May; and the cooling savings from 80% in May to 100% in March and October. An interesting result is the negative  $IESC_m$ -value in September, which means that the incorporation of PCM-drywalls in the room increases the cooling demand during this month. This means that some stored energy (for instance during summer) is released indoors and more 18% of energy is required for cooling.

During winter, the  $IESH_m$  and the  $IEST_m$  are both equal to 0.02 in January and February. The  $IEST_m$ -value is negative in December, which means that the annual optimized solution has a negative impact in the monthly energy demand. Another interesting result is the negative  $IESH_m$ -value in December, which means that the incorporation of PCM-drywalls increases the heating demand in 0.2%. In February, the  $IESC_m$  is equal to 1.0 and no energy is required for cooling due to PCMs. The  $IESC_m$  is not defined in January and December because no cooling is required. May is the month with the highest level of total energy savings, i.e. 2.04 kWh/m<sup>2</sup> (see Table 7). The negative values of the cooling energy savings in September indicates that an extra energy of 0.001 kWh/m<sup>2</sup> is required for cooling due to PCMs-drywalls incorporation. The same happens with the negative value of the heating savings in December. During this month more 0.04 kWh/m<sup>2</sup> are required for heating due to PCMs.

#### 4. Conclusion

In this paper, the impact of PCM-drywalls in the annual and monthly heating and cooling energy savings of an air-conditioned LSF residential single-zone room was evaluated based on the combination of an optimization model in GenOpt with dynamic energy simulations using EnergyPlus. A holistic approach is carried out to simulate more real-life conditions and the influence of several European climates.

It is concluded that an optimum solution incorporating PCM-drywalls can be found for each climate, leading to significant annual energy savings considering both cooling and heating energy demands. The results indicate an optimum thickness of the PCM-drywalls equal to 4.0 cm for all the case studies. The optimum melting peak temperature of the PCM is higher for the warmer climates: between 22 and 26 °C, against 18 to 24 °C for the colder climates. Inner surfaces with higher solar absorptance ( $\alpha = 0.9$ ) are better for colder climates and surfaces with lower solar absorptance ( $\alpha = 0.3$ ) are better for warmer climates.

It is also concluded that the energy savings effect is more evident for the warmer climates, where the total energy savings due to PCMs reach 46% and 62% for the Csa-Seville and Csb-Coimbra climates, respectively. It is also concluded that PCM-drywalls can be used to significantly reduce not only the cooling energy demand in the warmer climates, but also the heating energy demand. PCM-drywalls are also very attractive for colder climates (Dfb-Warsaw and Dfc-Kiruna), with a predominance of the heating energy demand reduction. However, the impact of PCMs in the total energy savings is not so significant for these climates (24% and 10% for the Dfb-Warsaw and Dfc-Kiruna climates, respectively). Regarding the other climates, Cfa-Milan, Cfb-Paris and Dfa-Bucharest, PCM-drywalls could be used to reduce the total energy demand for heating and cooling between 33% and 38%.

Regarding the monthly assessment, it is concluded that the optimum annual solution can increase the monthly energy performance of the LSF single-zone room for all the climates, except for the case of the Dfc-Kiruna climate. For this colder climate, the optimum solution faces a decrease in the energy efficiency during December. It is also concluded that the enhancement of the thermal capacity of the LSF envelope via PCM-drywalls changes the behaviour of the room every months.

The present study shows the importance of optimizing the incorporation of PCM-drywalls in an annual assessment basis rather than in a seasonal basis. Considering the Csa-Seville and the Csb-Coimbra climates, the total energy savings for heating and cooling are greater for the winter and swing seasons' months. For the Cfa-Milan and Dfa-Bucharest climates, the total energy savings are greater during the swing

seasons. For the remaining climates considered (Cfb-Paris, Dfb-Warsaw and Dfc-Kiruna), the total energy savings are greater for the summer and swing seasons' months.

The overall methodology proposed herein was focused on a single-zone room model. Therefore, the results can only be carefully extrapolated and generalized to more complex models and real multi-zone LSF buildings. Further work should be done to apply the presented methodology to more complex buildings by including more real-life indoor heat loads schedules, air infiltration models and heating/cooling systems operation. The study can also be extended to the optimization of the incorporation of real-commercialized PCM-drywalls (with different melting ranges) in real LSF buildings, for instance for retrofitting purposes.

### **Acknowledgement**

The first author acknowledges the support provided by the Portuguese Foundation for Science and Technology (FCT) under the PhD scholarship SFRH/BD/51640/2011.

### **References**

- [1] N. Soares, J.J. Costa, A.R. Gaspar, P. Santos, Review of passive PCM latent heat thermal energy storage systems towards buildings' energy efficiency, *Energy and Buildings* 59 (2013) 82-103.
- [2] D. Zhou, C.Y. Zhao, Y. Tian, Review on thermal energy storage with phase change materials (PCMs) in building applications, *Applied Energy* 92 (2012) 593-605.
- [3] V.A.A. Raj, R. Velraj, Review on free cooling of buildings using phase change materials, *Renewable and Sustainable Energy Reviews* 14 (9) (2010) 2819-29.
- [4] M.M. Farid, A.M. Khudhair, S. Ali, K. Razack, A review on phase change energy storage: materials and applications, *Energy Conversion and Management* 45 (2004) 1597-615.
- [5] A.M. Khudhair, M.M. Farid, A review on energy conservation in building applications with thermal storage by latent heat using phase change materials, *Energy Conversion and Management* 45 (2) (2004) 263-75.
- [6] N. Zhu, Z. Ma, S. Wang, Dynamic characteristics and energy performance of buildings using phase change materials: a review, *Energy Conversion and Management* 50 (12) (2009) 3169-81.
- [7] Y. Zhang, G. Zhou, K. Lin, Q. Zhang, H. Di, Application of latent heat thermal energy storage in buildings: state-of-the-art and outlook, *Building and Environment* 42 (6) (2007) 2197-209.

- [8] R. Baetens, B.P. Jelle, A. Gustavsen, Phase change materials for building applications: a state-of-the-art review, *Energy and Buildings* 42 (9) (2010) 1361-8.
- [9] E. Rodriguez-Ubinas, L. Ruiz-Valero, S. Vega, J. Neila, Applications of phase change material in highly energy-efficient houses, *Energy and Buildings* 50 (2012) 49-62.
- [10] E. Osterman, V.V. Tyagi, V. Butala, N.A. Rahim, U. Stritih, Review of PCM based cooling technologies for buildings, *Energy and Buildings* 49 (2012) 37-49.
- [11] V.V. Tyagi, D. Buddhi, PCM thermal storage in buildings: a state of art, *Renewable and Sustainable Energy Reviews* 11 (6) (2007) 1146-66.
- [12] A. Sharma, V.V. Tyagi, C.R. Chen, D. Buddhi, Review on thermal energy storage with phase change materials and applications, *Renewable and Sustainable Energy Reviews* 13 (2) (2009) 318-45.
- [13] F. Kuznik, D. David, K. Johannes, J.-J. Roux, A review on phase change materials integrated in building walls, *Renewable and Sustainable Energy Reviews* 15 (1) (2011) 379-91.
- [14] V.V. Tyagi, S.C. Kaushik, S.K. Tyagi, T. Akiyama, Development of phase change materials based microencapsulated technology for buildings: a review, *Renewable and Sustainable Energy Reviews* 15 (2) (2011) 1373-91.
- [15] L.F. Cabeza, A. Castell, C. Barreneche, A. de Gracia, A.I. Fernández, Materials used as PCM in thermal energy storage in buildings: a review, *Renewable and Sustainable Energy Reviews* 15 (3) (2011) 1675-95.
- [16] B. Zalba, J.M. Marín, L.F. Cabeza, H. Mehling, Review on thermal energy storage with phase change: materials, heat transfer analysis and applications, *Applied Thermal Engineering* 23 (3) (2003) 251-83.
- [17] D. David, F. Kuznik, J.-J. Roux, Numerical study of the influence of the convective heat transfer on the dynamical behaviour of a phase change material wall, *Applied Thermal Engineering* 31 (16) (2011) 3117-24.
- [18] F. Kuznik, J. Virgone, J. Noel, Optimization of a phase change material wallboard for building use, *Applied Thermal Engineering* 28 (11-12) (2008) 1291-8.
- [19] Y. Zhang, K. Lin, Y. Jiang, G. Zhou, Thermal storage and nonlinear heat-transfer characteristics of PCM wallboard, *Energy and Buildings* 40 (9) (2008) 1771-9.
- [20] G. Zhou, Y. Zhang, X. Wang, K. Lin, W. Xiao, An assessment of mixed type PCM-gypsum and shape-stabilized PCM plates in a building for passive solar heating, *Solar Energy* 81 (2007) 1351-60.
- [21] B.M. Diaconu, M. Cruceru, Novel concept of composite phase change material wall system for year-round thermal energy savings, *Energy and Buildings* 42 (10) (2010) 1759-72.

- [22] B.M. Diaconu, Thermal energy savings in buildings with PCM-enhanced envelope: influence of occupancy pattern and ventilation, *Energy and Buildings* 43 (1) (2011) 101-7.
- [23] D.A. Neeper, Thermal dynamics of wallboard with latent heat storage, *Solar Energy* 68 (5) (2000) 393-403.
- [24] L. Shilei, F. Guohui, Z. Neng, D. Li, Experimental study and evaluation of latent heat storage in phase change materials wallboards, *Energy and Buildings* 39 (10) (2007) 1088-91.
- [25] L. Shilei, Z. Neng, F. Guohui, Impact of phase change wall room on indoor thermal environment in winter, *Energy and Buildings* 38 (1) (2006) 18-24.
- [26] S. Scalat, D. Banu, D. Hawes, J. Paris, F. Haghghata, D. Feldman, Full scale thermal testing of latent heat storage in wallboard, *Solar Energy Materials and Solar Cells* 44 (1996) 46-61.
- [27] H. Liu, H.B. Awbi, Performance of phase change material boards under natural convection, *Building and Environment* 44 (9) (2009) 1788-93.
- [28] F. Kuznik, J. Virgone, J.-J. Roux, Energetic efficiency of room wall containing PCM wallboard: a full-scale experimental investigation, *Energy and Buildings* 40 (2) (2008) 148-56.
- [29] M. Ahmad, A. Bontemps, H. Sallée, D. Quenard, Experimental investigation and computer simulation of thermal behaviour of wallboards containing a phase change material, *Energy and Buildings* 38 (4) (2006) 357-66.
- [30] F. Kuznik, J. Virgone, Experimental investigation of wallboard containing phase change material: data for validation of numerical modeling, *Energy and Buildings* 41 (5) (2009) 561-70.
- [31] J. Koo, H. So, S.W. Hong, H. Hong, Effects of wallboard design parameters on the thermal storage in buildings, *Energy and Buildings* 43 (8) (2011) 1947-51.
- [32] P. Schossig, H.-M. Henning, S. Gschwander, T. Haussmann, Micro-encapsulated phase-change materials integrated into construction materials, *Solar Energy Materials and Solar Cells* 89 (2-3) (2005) 297-306.
- [33] C. Chen, H. Guo, Y. Liu, H. Yue, C. Wang, A new kind of phase change material (PCM) for energy-storing wallboard, *Energy and Buildings* 40 (5) (2008) 882-90.
- [34] M. Ahmad, A. Bontemps, H. Sallée, D. Quenard, Thermal testing and numerical simulation of a prototype cell using light wallboards coupling vacuum isolation panels and phase change material, *Energy and Buildings* 38 (6) (2006) 673-81.
- [35] A.K. Athienitis, C. Liu, D. Hawes, D. Banu, D. Feldman, Investigation of the thermal performance of a passive solar test-room with wall latent heat storage, *Building and Environment* 5 (1997) 405-10.

- [36] A.M. Borreguero, M.L. Sánchez, J.L. Valverde, M. Carmona, J.F. Rodríguez, Thermal testing and numerical simulation of gypsum wallboards incorporated with different PCMs content, *Applied Energy* 88 (3) (2011) 930-7.
- [37] F. Kuznik, J. Virgone, K. Johannes, In-situ study of thermal comfort enhancement in a renovated building equipped with phase change material wallboard, *Renewable Energy* 36 (5) (2011) 1458-62.
- [38] I. Mandilaras, M. Stamatiadou, D. Katsourinis, G. Zannis, M. Founti, Experimental thermal characterization of a Mediterranean residential building with PCM gypsum board walls, *Building and Environment* 61 (2013) 93-103.
- [39] M. Wetter, J. Wright, A comparison of deterministic and probabilistic optimization algorithms for nonsmooth simulation-based optimization, *Building and Environment* 39 (8) (2004) 989-99.
- [40] E. Asadi, M.G. da Silva, C.H. Antunes, L. Dias, A multi-objective optimization model for building retrofit strategies using TRNSYS simulations, GenOpt and MATLAB, *Building and Environment* 56 (2012) 370-8.
- [41] A. Hasan, M. Vuolle, K. Sirén, Minimisation of life cycle cost of a detached house using combined simulation and optimisation, *Building and Environment* 43 (12) (2008) 2022-34.
- [42] M. Fesanghary, S. Asadi, Z.W. Geem, Design of low-emission and energy-efficient residential buildings using a multi-objective optimization algorithm, *Building and Environment* 49 (2012) 245-50.
- [43] GenOpt 3.1.0, Generic optimization program. <http://gundog.lbl.gov/GO/>, 2013.
- [44] EnergyPlus 8.0.0, Energy simulation software. <http://apps1.eere.energy.gov/buildings/energyplus/>, 2013.
- [45] ESP-r. <http://www.esru.strath.ac.uk/Programs/ESP-r.htm>, 2013.
- [46] TRNSYS 17, A transient systems simulation program. <http://sel.me.wisc.edu/trnsys/>, 2013.
- [47] M. Ibáñez, A. Lázaro, B. Zalba, L.F. Cabeza, An approach to the simulation of PCMs in building applications using TRNSYS, *Applied Thermal Engineering* 25 (11-12) (2005) 1796-807.
- [48] G. Evola, L. Marletta, F. Sicurella, A methodology for investigating the effectiveness of PCM wallboards for summer thermal comfort in buildings, *Building and Environment* 59 (2013) 517-27.
- [49] P.C. Tabares-Velasco, C. Christensen, M. Bianchi, Verification and validation of EnergyPlus phase change material model for opaque wall assemblies, *Building and Environment* 54 (2012) 186-96.
- [50] P. Tabares-Velasco, Energy impacts of nonlinear behavior of PCM when applied into building envelope, in: ASME 2012 6th International Conference on Energy Sustainability & 10th Fuel Cell Science, Engineering and Technology Conference, San Diego, California, 2012.

- [51] C.O. Pedersen, Advanced zone simulation in EnergyPlus: incorporation of variable properties and phase change material (PCM) capability, in: Proceedings of Building Simulation 2007, Beijing, China, 2007.
- [52] P. Hoes, M. Trecka, J.L.M. Hensen, B.H. Bonnema, Investigating the potential of a novel low-energy house concept with hybrid adaptable thermal storage, *Energy Conversion and Management* 52 (6) (2011) 2442-7.
- [53] D. Heim, J.A. Clarke, Numerical modelling and thermal simulation of PCM-gypsum composites with ESP-r, *Energy and Buildings* 36 (8) (2004) 795-805.
- [54] D. Heim, Isothermal storage of solar energy in building construction, *Renewable Energy* 35 (4) (2012) 788-96.
- [55] N.T.A. Fernandes, V.A.F. Costa, Use of phase-change materials as passive elements for climatization purposes in summer: the Portuguese case, *International Journal of Green Energy* 6 (3) (2009) 302-11.
- [56] M. Koschenz, B. Lehmann, Development of a thermally activated ceiling panel with PCM for application in lightweight and retrofitted buildings, *Energy and Buildings* 36 (6) (2004) 567-78.
- [57] F. Kuznik, J. Virgone, K. Johannes, Development and validation of a new TRNSYS type for the simulation of external building walls containing PCM, *Energy and Buildings* 42 (7) (2010) 1004-9.
- [58] A. Bontemps, M. Ahmad, K. Johannès, H. Sallée, Experimental and modelling study of twin cells with latent heat storage walls, *Energy and Buildings* 43 (9) (2011) 2456-61.
- [59] M. Wetter, GenOpt: Generic Optimization program, user manual version 3.1.0, Lawrence Berkeley National Laboratory, 2011.
- [60] R. Eberhart, J. Kennedy, A new optimizer using particle swarm theory, in: Sixth International Symposium on Micro Machine and Human Science, Nagoya, Japan, 1995, pp. 39-43.
- [61] J. Kennedy, R. Eberhart, Particle swarm optimization, in: IEEE International Conference on Neural Networks, volume IV, Perth, Australia, 1995, pp. 1942-1948.
- [62] M. Kottek, J. Grieser, C. Beck, B. Rudolf, F. Rubel, World Map of the Köppen-Geiger climate classification updated, *Meteorologische Zeitschrift* 15 (3) (2006) 259-63.
- [63] S. Cao, A. Gustavsen, S. Uvsløkk, B.P. Jelle, J. Gilbert, J. Maunuksela, The Effect of Wall-Integrated Phase Change Material Panels on the Indoor Air and Wall Temperature – Hot box Experiments, in: Proceedings of Renewable Energy Research Conference 2010, Trondheim, Norway, 2010.
- [64] ANSI/ASHRAE Standard 140-2004, Standard method of test for the evaluation of building energy analysis computer programs, GA: American Society of Heating, Refrigerating, and Air-Conditioning Engineers, Atlanta, 2004.



- [65] S. Doran, M. Gorgolewski, U-values for light steel-frame construction, BRE Digest 465, Building Research Establishment, UK, 2002.
- [66] Concerted action EPBD, Implementing the Energy Performance of Buildings Directive (EPBD) - Featuring Country Reports 2010, Brussels, April 2011. 2011.
- [67] A.P. Gomes, H.A. de Souza, A. Tribess, Impact of thermal bridging on the performance of buildings using Light Steel Framing in Brazil, Applied Thermal Engineering 52 (1) (2013) 84-9.
- [68] M. Gorgolewski, Developing a simplified method of calculating U-values in light steel framing, Building and Environment 42 (1) (2007) 230-6.
- [69] European Committee for Standardization, Building components and building elements - thermal resistance and thermal transmittance - calculation method, EN ISO 6946:1996.

Table 1. Characterization of the European climates: Köppen-Geiger climate classification and description.  
 Climates provided by the International Weather for Energy Calculation (IWEC) files [44].

Location	Köppen-Geiger classification	Climate description [44]
Seville, Spain	Csa	Mediterranean climate (dry hot summer, mild winter, lat. 30-45°N)
Coimbra, Portugal	Csb	Mediterranean climate (dry warm summer, mild winter, lat. 30-45°N)
Milan, Italy	Cfa	Humid subtropical (mild with no dry season, hot summer, lat. 20-35°N)
Paris, France	Cfb	Marine west coastal (warm summer, mild winter, rain all year, lat. 35-60°N)
Bucharest, Romania	Dfa	Humid continental (hot summer, cold winter, no dry season, lat. 30-60°N)
Warsaw, Poland	Dfb	Moist continental (warm summer, cold winter, no dry season, lat. 30-60°N)
Kiruna, Sweden	Dfc	Subarctic (cool summer, severe winter, no dry season, lat. 50-70°N)

Table 2. Thermophysical properties of the building components.

Material	$k$ (W/m K)	$c_p$ (J/kg K)	$\rho$ (kg/m <sup>3</sup> )
EIFS finish	1.150	1500	1050
EPS	0.040	1400	15
XPS	0.034	1400	35
Rockwool	0.040	840	30
OSB	0.130	1700	650
Plasterboard	0.250	1000	900
Mortar slab	0.880	896	2800
Cast concrete	0.380	1000	1200
Gravel	2.800	800	2500
Interior finishing	0.170	1400	1200
Steel	50.000	450	7800

Table 3. Reference  $U$ -values (and correspondent insulation thicknesses) of the exterior opaque elements and windows for the different climates according to the building regulations of each country.

	<b>Csa</b>	<b>Csb</b>	<b>Cfa</b>	<b>Cfb</b>	<b>Dfa</b>	<b>Dfb</b>	<b>Dfc</b>
	Seville	Coimbra	Milan	Paris	Bucharest	Warsaw	Kiruna
$U_{ref,wall}$ (W/m <sup>2</sup> K)	0.82	0.70	0.34	0.45	0.57	0.30	0.18
$U_{ref,roof}$ (W/m <sup>2</sup> K)	0.45	0.50	0.30	0.28	0.20	0.25	0.13
$U_{ref,win}$ (W/m <sup>2</sup> K)	5.20	4.30	2.20	2.00	1.30	1.70	1.30
$e_{ins,wall}$ (mm)	0.60	6.00	53.00	30.00	15.50	65.00	140.00
$e_{ins,roof}$ (mm)	5.00	0.50	30.00	38.00	73.00	47.00	150.00

Table 4. Thermal conductivity of the equivalent homogeneous layer materials for each climate.

		<b>Csa</b>	<b>Csb</b>	<b>Cfa</b>	<b>Cfb</b>	<b>Dfa</b>	<b>Dfb</b>	<b>Dfc</b>
		Seville	Coimbra	Milan	Paris	Bucharest	Warsaw	Kiruna
Exterior walls	$k_{eq,wall}$ (W/m K)	0.114	0.107	0.077	0.086	0.096	0.073	0.061
Exterior roof	$k_{eq,roof}$ (W/m K)	0.140	0.147	0.114	0.109	0.092	0.104	0.077
Partition wall	$k_{eq,part}$ (W/m K)	0.112	0.112	0.112	0.112	0.112	0.112	0.112

Table 5. Values of the independent variables that yield better performance for each climate, i.e.  $x^* =$ 

$$\{S_j, W_k, E_l, N_m, C_p\}_{opt.}$$

		<b>Csa</b>	<b>Csb</b>	<b>Cfa</b>	<b>Cfb</b>	<b>Dfa</b>	<b>Dfb</b>	<b>Dfc</b>
		Seville	Coimbra	Milan	Paris	Bucharest	Warsaw	Kiruna
Partition northern wall $N_m$	$e_{PCM}$ (cm)	4.0	4.0	4.0	4.0	4.0	4.0	4.0
	$T_{pm}$ (°C)	24.0	22.0	22.0	22.0	22.0	22.0	20.0
	$\alpha$	0.3	0.3	0.3	0.9	0.3	0.9	0.9
Exterior western wall $W_k$	$e_{PCM}$ (cm)	4.0	4.0	4.0	4.0	4.0	4.0	4.0
	$T_{pm}$ (°C)	26.0	24.0	24.0	22.0	24.0	22.0	20.0
	$\alpha$	0.3	0.3	0.9	0.9	0.9	0.9	0.9
Exterior eastern wall $E_l$	$e_{PCM}$ (cm)	4.0	4.0	4.0	4.0	4.0	4.0	4.0
	$T_{pm}$ (°C)	26.0	24.0	24.0	24.0	24.0	22.0	18.0
	$\alpha$	0.3	0.3	0.9	0.9	0.9	0.9	0.9
Exterior southern wall $S_j$	$e_{PCM}$ (cm)	4.0	4.0	4.0	4.0	4.0	4.0	4.0
	$T_{pm}$ (°C)	26.0	24.0	24.0	22.0	24.0	22.0	20.0
	$\alpha$	0.3	0.3	0.3	0.9	0.3	0.9	0.9
Exterior ceiling $C_p$	$e_{PCM}$ (cm)	4.0	4.0	4.0	4.0	4.0	4.0	4.0
	$T_{pm}$ (°C)	26.0	24.0	24.0	22.0	22.0	22.0	24.0
	$\alpha$	0.3	0.3	0.3	0.3	0.3	0.3	0.3

Table 6. Annual heating/cooling energy demands of the reference and the PCM-drywalls enhanced air-conditioned LSF rooms for each climate considered, and annual energy savings considering the optimized

$$\text{solution } x^* = \{S_j, W_k, E_l, N_m, C_p\}_{opt.}$$

Annual energy demands (kWh/m <sup>2</sup> year)		<b>Csa</b>	<b>Csb</b>	<b>Cfa</b>	<b>Cfb</b>	<b>Dfa</b>	<b>Dfb</b>	<b>Dfc</b>
		Seville	Coimbra	Milan	Paris	Bucharest	Warsaw	Kiruna
Cooling	$E_{cool,ref}$	78.45	40.37	27.11	14.21	32.73	9.92	3.76
	$E_{cool,PCM}$	44.52	15.58	14.81	4.02	16.32	2.58	0.48
	Savings	33.94	24.78	12.30	10.18	16.40	7.34	3.28
Heating	$E_{heat,ref}$	4.65	5.64	27.56	30.67	33.64	47.31	98.96
	$E_{heat,PCM}$	0.36	1.69	21.70	24.77	25.15	40.96	92.38
	Savings	4.30	3.95	5.86	5.90	8.49	6.34	6.58
Total	$E_{tot,ref}$	83.10	46.01	54.67	44.88	66.37	57.23	102.72
	$E_{tot,PCM}$	44.87	17.27	36.51	28.80	41.47	43.55	92.86
	Savings	38.23	28.74	18.16	16.08	24.90	13.68	9.86

Table 7. Monthly heating/cooling energy savings for the analysed climates considering the optimized

$$\text{solution } x^* = \{S_p, W_k, E_b, N_m, C_p\}_{\text{opt.}}$$

Climate	Energy savings (kWh/m <sup>2</sup> month)	Jan.	Feb.	Mar.	Apr.	May	Jun.	Jul.	Aug.	Sep.	Oct.	Nov.	Dec.
<b>Csa</b> Seville	Cooling	3.04	3.43	3.70	2.22	2.93	2.24	2.82	2.50	2.33	3.31	2.77	2.63
	Heating	1.39	0.72	0.40	0.29	0.00	0.00	0.00	0.00	0.00	0.01	0.57	0.92
	Total	4.43	4.15	4.10	2.51	2.93	2.24	2.82	2.50	2.34	3.32	3.33	3.55
<b>Csb</b> Coimbra	Cooling	2.02	1.53	2.51	2.27	1.98	2.04	2.33	2.29	2.11	3.05	1.06	1.58
	Heating	0.86	0.67	0.49	0.18	0.05	0.00	0.00	0.01	0.00	0.03	0.79	0.88
	Total	2.88	2.20	3.00	2.46	2.04	2.05	2.33	2.29	2.11	3.08	1.84	2.46
<b>Cfa</b> Milan	Cooling	0.08	0.35	1.52	1.65	1.83	1.41	1.18	1.03	0.82	2.18	0.25	0.01
	Heating	1.20	1.14	0.87	0.49	0.02	0.01	0.00	0.00	0.04	0.29	1.06	0.75
	Total	1.27	1.49	2.39	2.14	1.85	1.42	1.18	1.03	0.87	2.47	1.31	0.76
<b>Cfb</b> Paris	Cooling	0.26	0.29	0.33	1.11	1.31	1.08	1.77	1.23	0.48	1.83	0.49	0.00
	Heating	1.00	1.08	0.67	0.43	0.05	0.03	0.01	0.00	0.24	0.65	1.24	0.51
	Total	1.25	1.37	1.00	1.54	1.36	1.10	1.78	1.23	0.72	2.48	1.72	0.51
<b>Dfa</b> Bucharest	Cooling	0.03	1.11	1.98	2.53	1.61	1.57	1.87	1.38	1.10	2.43	0.55	0.25
	Heating	1.24	1.73	1.54	0.41	0.00	0.00	0.00	0.03	0.29	0.89	1.15	1.22
	Total	1.27	2.84	3.52	2.94	1.62	1.57	1.87	1.41	1.39	3.32	1.70	1.47
<b>Dfb</b> Warsaw	Cooling	0.00	0.09	0.34	1.42	1.37	0.66	1.37	1.13	0.24	0.52	0.16	0.04
	Heating	0.44	0.86	1.07	0.98	0.00	0.03	0.04	0.01	0.77	0.84	0.74	0.56
	Total	0.44	0.95	1.41	2.40	1.37	0.69	1.41	1.13	1.01	1.36	0.90	0.60
<b>Dfc</b> Kiruna	Cooling	0.00	0.02	0.15	0.84	1.26	0.31	0.61	0.02	-0.00	0.07	0.00	0.00
	Heating	0.47	0.30	1.28	0.59	0.78	0.66	0.14	0.74	0.40	0.72	0.55	-0.04
	Total	0.47	0.31	1.43	1.43	2.04	0.97	0.75	0.77	0.40	0.78	0.55	-0.04

**Fig.1.** (a) Enthalpy-temperature and (b) thermal conductivity-temperature functions for the reference PCM-drywall and for other six hypothetical materials defined.\*Data for DuPont™ Energain® PCM product obtained from differential scanning calorimeter (DSC) measurements with a heating rate of 0.05 °C/min [63].

**Fig.2.** Sketch of the case study living room facing the south facade.

**Fig.3.** Occupancy, lighting and equipment schedules during (a) weekdays and (b) weekends.

**Fig.4.** Cross-section of the construction elements considered in the model: (a) exterior wall, (b) roof, (c) slab-on-grade and (d) partition wall.

**Fig.5.** Annual heating and cooling energy demands for both the reference and the PCMenhanced rooms for each climate. Indices of annual energy savings for each climate considering the optimized solution  $x^* = \{S_j, W_k, E_l, N_m, C_p\}_{\text{opt}}$ .

**Fig.6.** Monthly heating and cooling energy demands for both the reference and the PCMenhanced rooms for the (a) Csa-Seville, (b) Csb-Coimbra, (c) Cfa-Milan, (d) Cfb-Paris, (e) Dfa-Bucharest, (f) Dfb-Warsaw and (g) Dfc-Kiruna climates. Indices of energy savings for each month considering the optimized solution  $x^* = \{S_j, W_k, E_l, N_m, C_p\}_{\text{opt}}$  for each climate.

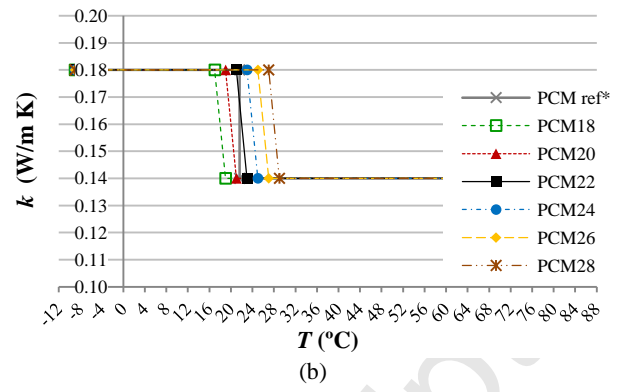
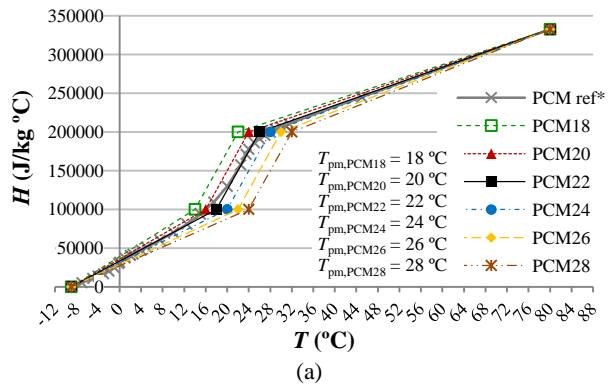
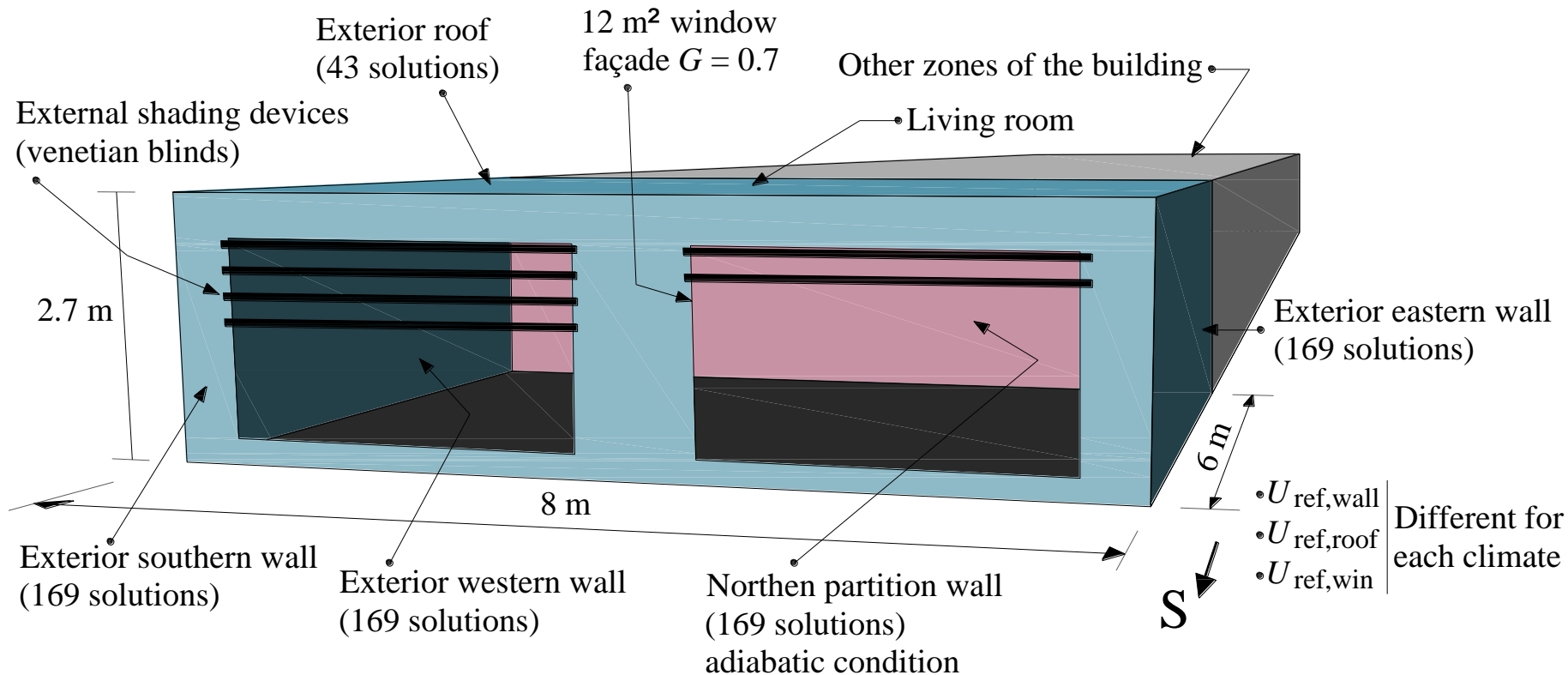
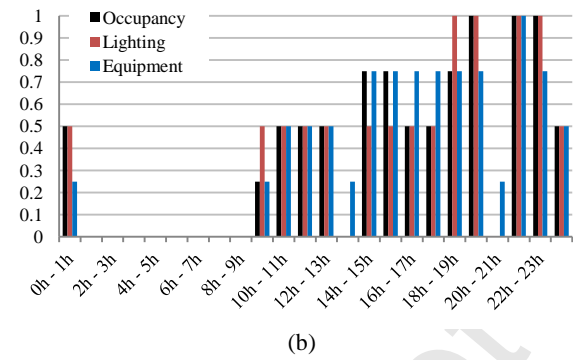
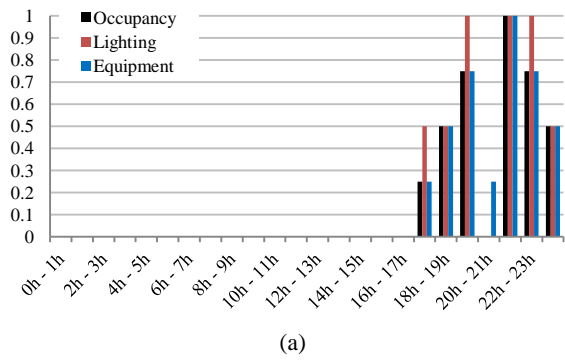


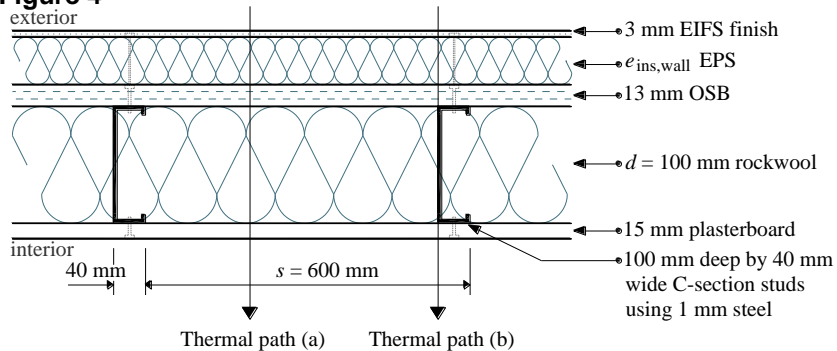
Figure 2



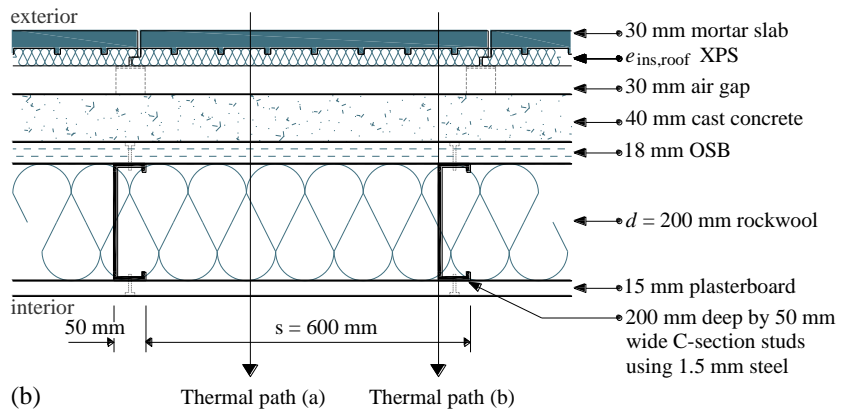


Accepted Manuscript

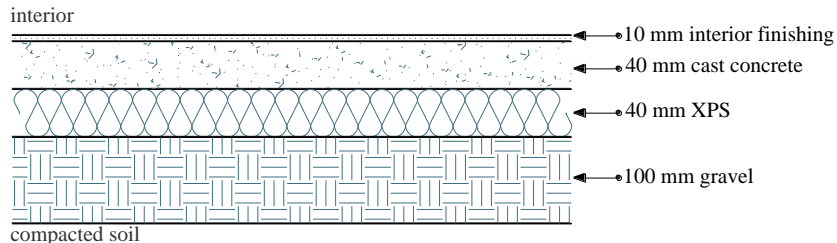


**Figure 4**

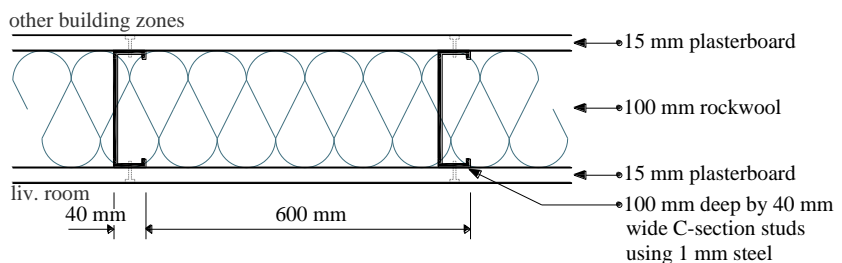
(a)



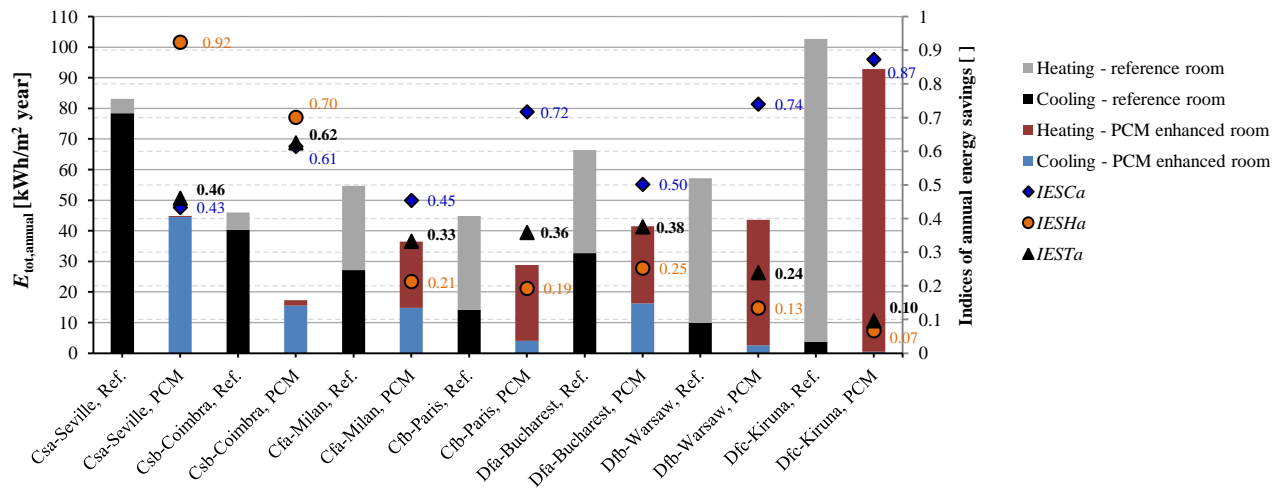
(b)



(c)



(d)



Accepted Manuscript

